THERMAL STRESSES IN STEAM-CURED CONCRETE

by

GY. BALÁZS—M. BERÉNYI—B. SZENTIVÁNYI
Department of Building Materials, Technical University, Budapest

(Received February 15, 1973)
Presented by Prof. Dr. J. TALABÉR

Steam-curing is the most important means to accelerate hardening of precast concrete and reinforced concrete units. Steam-curing is controlled by steam-curing diagrams. It is obvious from the diagrams in Fig. 1 that the steam-curing procedure has four distinct stages: self-curing, heating, isothermal curing and cooling periods. Risks of thermal stresses arise especially in the cooling period. Namely the concrete is still plastic when heated, whereas in the cooling period — in case of large-size concrete units with uneven temperature distribution — tensile stresses develop because for some time the temperature in the concrete is higher than the ambient temperature, likely to cause cracks in the concrete. Such cracks were observed e.g. in the first tubbing elements for the Metro of Budapest, as soon as removed from the steam-curing space; the steam-curing technology being developed for smaller units [1]. The aim of this project was to determine thermal stresses developing in the cooling period.

A procedure was developed to determine the temperature distribution, responsible for thermal stresses in beams of arbitrary cross-section. As beams are much longer than wide, the longitudinal temperature distribution may be considered as uniform. The temperature distribution in cross-sections normal to the longitudinal axis is described by the two-dimensional form of the Fourier differential equation:

$$\frac{\partial \Phi}{\partial t} = \frac{\lambda}{c_b \gamma_b} \left(\frac{\partial^2 \Phi}{\partial x^2} + \frac{\partial^2 \Phi}{\partial y^2} \right) + \frac{C \cdot Q_c}{c_b \gamma_b}$$

where Φ = the unknown temperature function,
t = time
λ = conductivity coefficient of the concrete
c_b = specific temperature of the concrete
γ_b = concrete density
C = cement content
Q_c = heat released by setting cement of unit weight per unit time.

Applying the so-called Newton cooling law as boundary condition:

$$\frac{\partial \Phi}{\partial n} = - \frac{\alpha}{\lambda} (\Phi - \varphi)$$

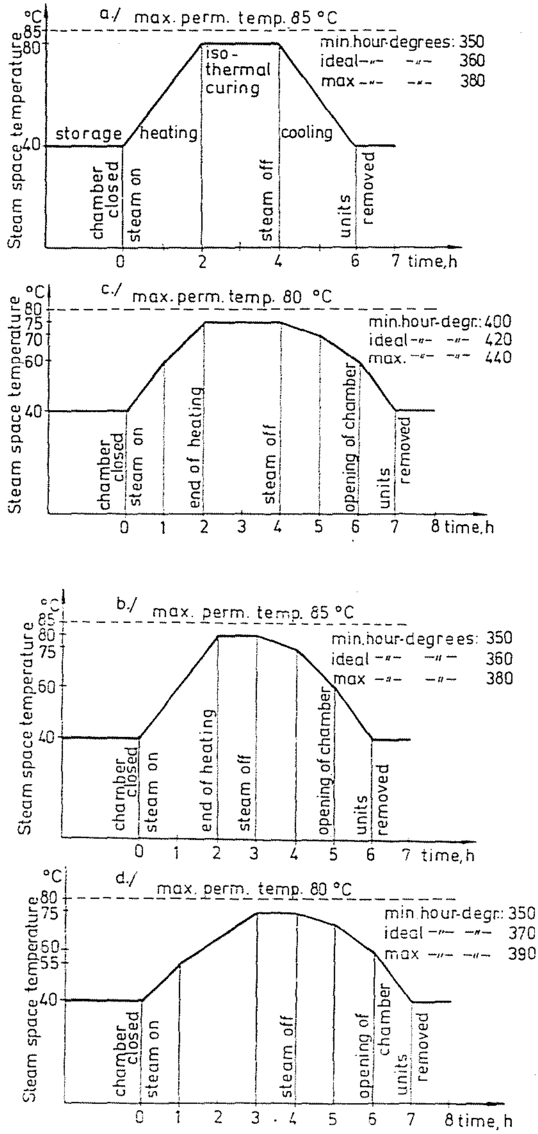

Fig. 1. Steam-curing diagrams used at present in the factory for: *a)* Beam F (cement C 500, hour/degrees: 360); *b)* Precast hall units, column, roof slab EP 12, for 12 m main truss beam and reinforced columns (cement C 500, hour/degrees: 360); *c)* Beam E (cement C 500, hour/ degrees: 420); *d)* Floor units PK, PS (cements C 500, C 600; hour/degrees: 370)

where $\frac{\partial \Phi}{\partial n}$ is the derivative of the temperature function normal to the boundary

α heat transfer coefficient between the concrete and the ambient air space

φ ambient temperature.

Variation in time of the thermal material characteristics was omitted in the calculations. The Fourier differential equation was solved by a numerical approximation method, i.e., the method of finite elements. The beam cross-section was divided into arbitrary triangular parts and the corner point values of the temperature function in each time interval were considered as unknown. The temperature within each triangle can be given at every time as a function of these unknowns and the co-ordinates x and y. The three parameters of the condition function

$$\Phi = \alpha_1 + \alpha_2 x + \alpha_3 y$$

presumed for the temperature distribution within each triangle are easily expressed in terms of the three corner temperature values. Solution of the Fourier differential equation can be retraced to the determination of the following integral expression, yielding the minimum of function Φ.

$$I(\Phi) = \iint\limits_{T} \left\{ \frac{1}{2} \cdot \frac{\lambda}{c_b \gamma_b} \left[\left(\frac{\partial \Phi}{\partial x} \right)^2 + \left(\frac{\partial \Phi}{\partial y} \right)^2 \right] - \left[\frac{C \cdot Q_c}{c_c \gamma_b} - \frac{\partial \Phi}{\partial t} \right] \Phi \, dx \, dy . \right.$$

Above can be proved by the variation calculus method.

It follows from the minimizing condition that forming derivatives with respect to the corner values of this integral expression within each element, and summing the derivatives pertaining to one nodal value, the following inear differential equation system is obtained:

$$\mathbf{H} \cdot \mathbf{\Phi} + \mathbf{P} \left[\frac{\partial \mathbf{\Phi}}{\partial t} \right] + \mathbf{F} = 0 .$$

Supposing at the starting time the temperature of each point to be known, the vector $\left[\frac{\partial \mathbf{\Phi}}{\partial t} \right]_{t=0}$ pertaining to time $t = 0$ is determined. Supposing variation of $\frac{\partial \mathbf{\Phi}}{\partial t}$ to be linear within each period Δt, the differential equation system can be solved by stepwise integration. Boundary conditions were taken into account by modifying the "rigidity" matrix **H** and the load vector **F**.

In computing thermal stresses, the customary simplifications of elasticity were used. (The concrete is homogeneous, isotropic, follows the Hooke's law and the Bernoulli—Navier hypothesis.) Modulus of elasticity of the concrete was considered constant in the relatively short cooling interval and the effect of deformation was also neglected. For reinforced beams, approximations of the first stress condition were used. The instationary temperature field creates a stress condition changing as a function of time. According to the Duhamel hypothesis it may be supposed that the acceleration effect can be disregarded and the stress condition changing with time can be considered as a succession of equilibrium positions. The principle applied to determine the thermal stresses was to consider as first approximation the beam as clamped at both ends, each cross-section being in the condition of plane strain. Then on the stresses at both ends of the beam a linear stress distribution is superimposed, balancing a force system of longitudinal stresses at the beam ends, determined from the condition of plane strain. Thereby the condition is satisfied that the beam is not supported at its ends, and the local disturbances resulting from the different distribution of the two force systems vanish in the relatively small region of the beam end, in conformity with the Saint Venant principle.

The stresses were also calculated by the finite element method. The triangular division applied in the determination of temperature distribution was used; the elements were assumed to be connected at the corner points only and the nodal displacements became the basic unknown parameters of the problem. (In this way the continuum problem was traced back to the analysis of a planar structure by the displacement method.) The temperature within each triangle was supposed to be constant, and taken as the arithmetic average of the corner point values. The condition functions considered linear within each element were expressed, similarly to the temperature distribution, as nodal values vs. x and y. Then expressing the potential energy minimum of the whole system a linear equation system was obtained for determining the nodal displacement values. From these, the stresses of the plane deformation condition are easy to calculate.

The inverse of the force system of longitudinal stresses resulting from the plane strain condition

$$\sigma'_{z\Delta} = \nu(\sigma_x + \sigma_y) - E\alpha_b \cdot \Phi_\Delta$$

is reduced to the origin of the co-ordinate system and the matrix equation between deformations and strains is written as

$$E \cdot \begin{bmatrix} I_x & C_{xy} & S_x \\ C_{xy} & I_y & S_y \\ S_x & S_y & F \end{bmatrix} \begin{bmatrix} \varphi_x \\ \varphi_y \\ w_z \end{bmatrix} = \begin{bmatrix} M_x \\ M_y \\ P \end{bmatrix}$$

according to the excentric tension, where F is the cross-section area; S_x, S_y its static moments; I_x and I_y secondary moments along axes x and y; C_{xy} is the centrifugal moment along axes x and y; E being the modulus of elasticity.

Solving it for the displacements, the stress superimposed on the longitudinal stress obtained from the condition of plane strain is:

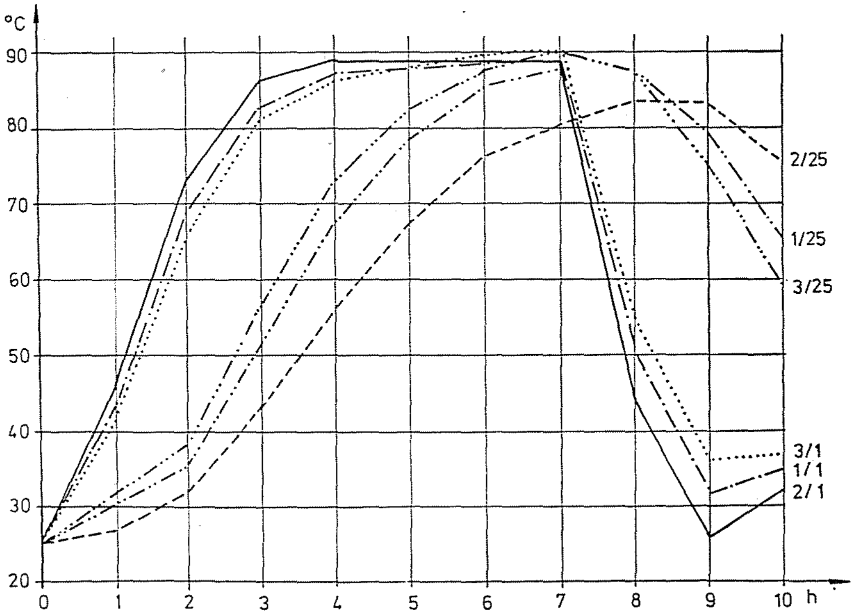

Fig. 2. Concrete temperature development in steam-curing for different heat conductivities (1. $\lambda = 1.8$ kcal/m h °C, 2. $\lambda = 0.9$ kcal/m h °C, 3. $\lambda = 2.7$ kcal/m h °C), on the beam surface (point No. 1) and in the centre of the beam (point No. 25)

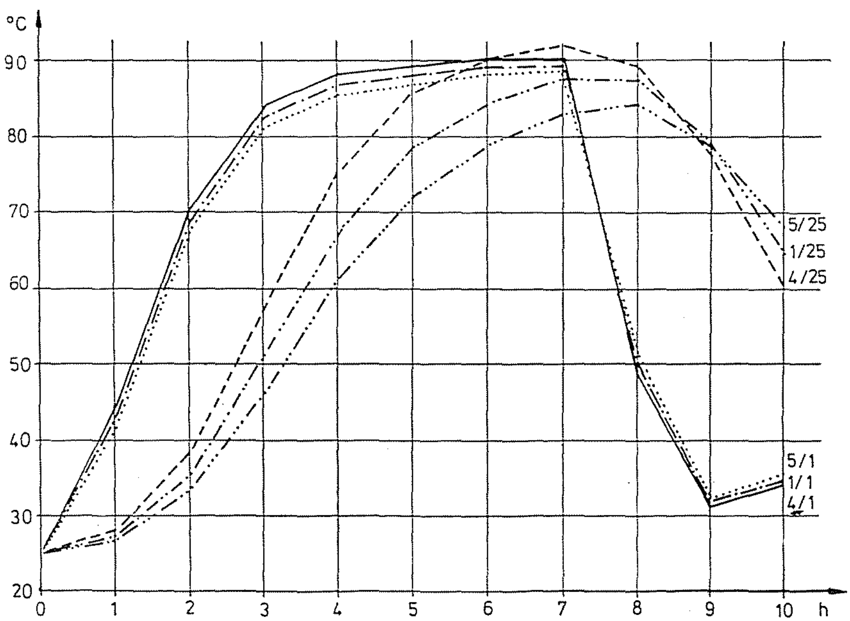

Fig. 3. Concrete temperature development in steam-curing for different specific heat values (1. $c_b = 0.23$ kcal/kg °C; 4. $c_b = 0.19$ kcal/kg °C; 5. $c_b = 0.27$ kcal/kg °C) at the corner point of the beam (point No. 1) and in the beam centre (point No. 25)

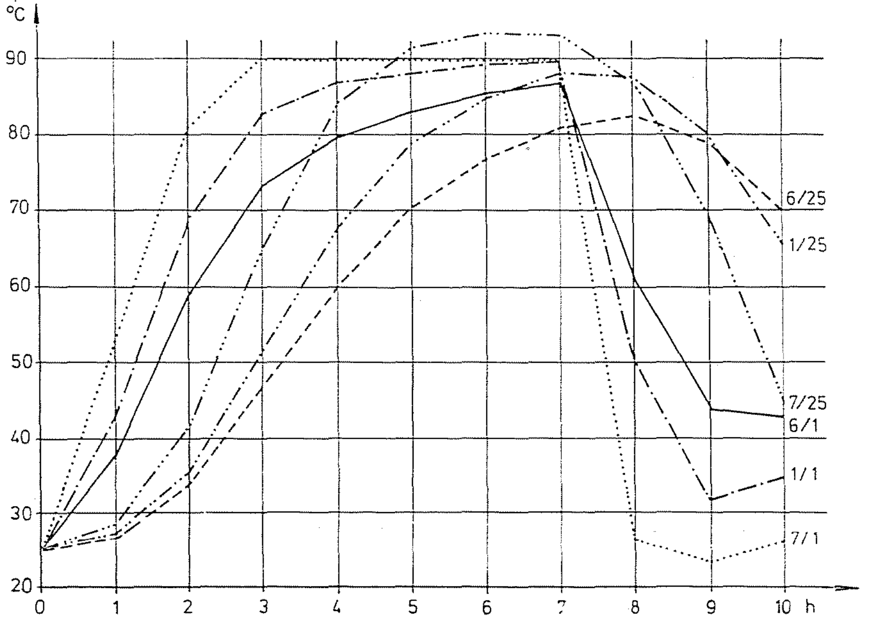

Fig. 4. Concrete temperature development in steam-curing for different heat transfer coefficients (1. $\alpha = 20$ kcal/m^2 h °C; 6. $\alpha = 10$ kcal/m^2 h °C; 7. $\alpha = 200$ kcal/m^2 h °C) at the external corner point of the beam (point No. 1) and in the beam centre (point No. 25)

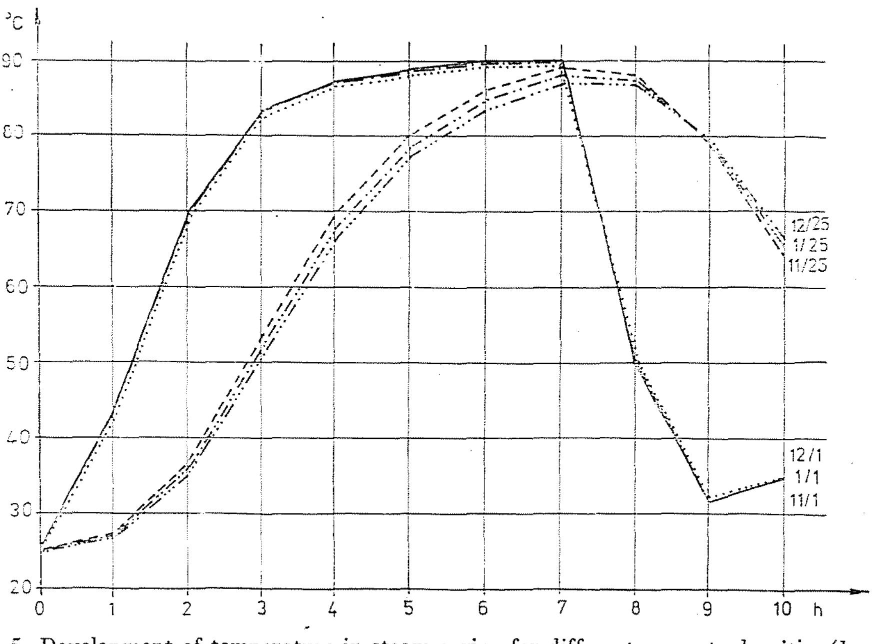

Fig. 5. Development of temperature in steam-curing for different concrete densities (1. $\gamma =$ 2400 kg/m^3; 11. $\gamma = 2300$ kg/m^3; 12. $\gamma = 2500$ kg/m^3) at the corner point of the beam (point No. 1) and in the beam centre (point No. 25)

$$\sigma''_{z\Delta} = E\,(\varphi_x y^* + \varphi_y \cdot x^* + w_z)$$

x^*, y^* being co-ordinates of the triangle's centre of gravity.

Based on the above principles a computer simulation program in FORTRAN language was developed for a SIEMENS 4004 computer. The

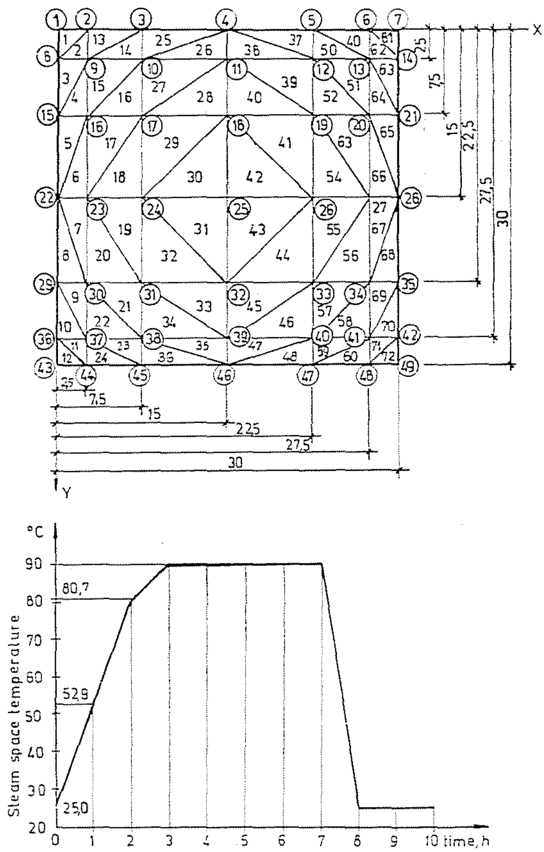

Fig. 6. Division and steam-curing diagram used for testing the effect of material characteristics

tested beam may be of any cross-section, the accidentally curved boundaries can be substituted by a straight-sided polygon. The net of arbitrary triangles can be discretionally made denser at the place of expected stress maxima. The steam-curing period was divided into identical time intervals Δt. The program can cope with 360 dividing points, 600 triangular elements and 200 time intervals. The Concrete and Reinforced Concrete Works granted 5 hours running time for the program.

To determine the input data of the program, both the thermal characteristics of the concrete and the development of hydration heat of the cement had to be examined.

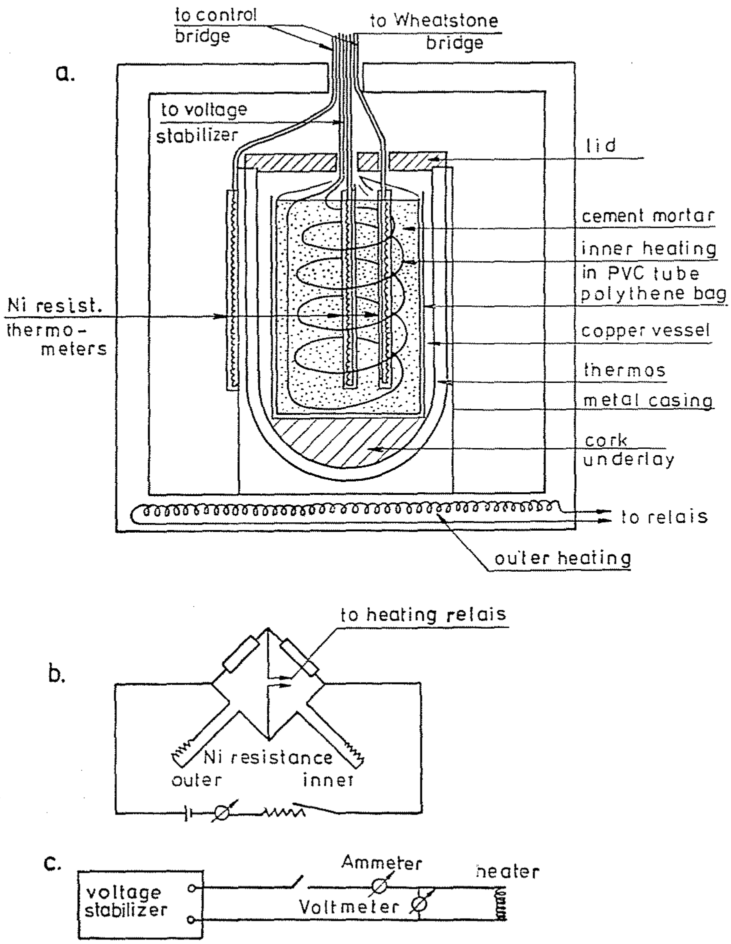

Fig. 7. Sketch of the testing equipment for measuring cement hydration heat and circuit diagram, *a)* Testing equipment; *b)* Control bridge of outer heating; *c)* Control circuit diagram

Thermal characteristics reported in the literature are rather scattered. Since no relevant tests have been made, the use of statistical relationships obtained from the great many tests described in literature was endeavoured. They yield the thermal features of the concrete as a function of the composition, the temperature, etc., neglecting the less important effects. To determine the conductivity and the specific heat, the formula

$$\lambda = \Sigma G_v \cdot f_1 \, ; \quad c_b = \Sigma G_v \cdot f_2$$

of the US Bureau of Reclamation was used, G_v indicating the percentage by weight of concrete components, f_1 and f_2 coefficients tabulated for cement and the different aggregates vs. concrete temperature mean. In the heat trans-

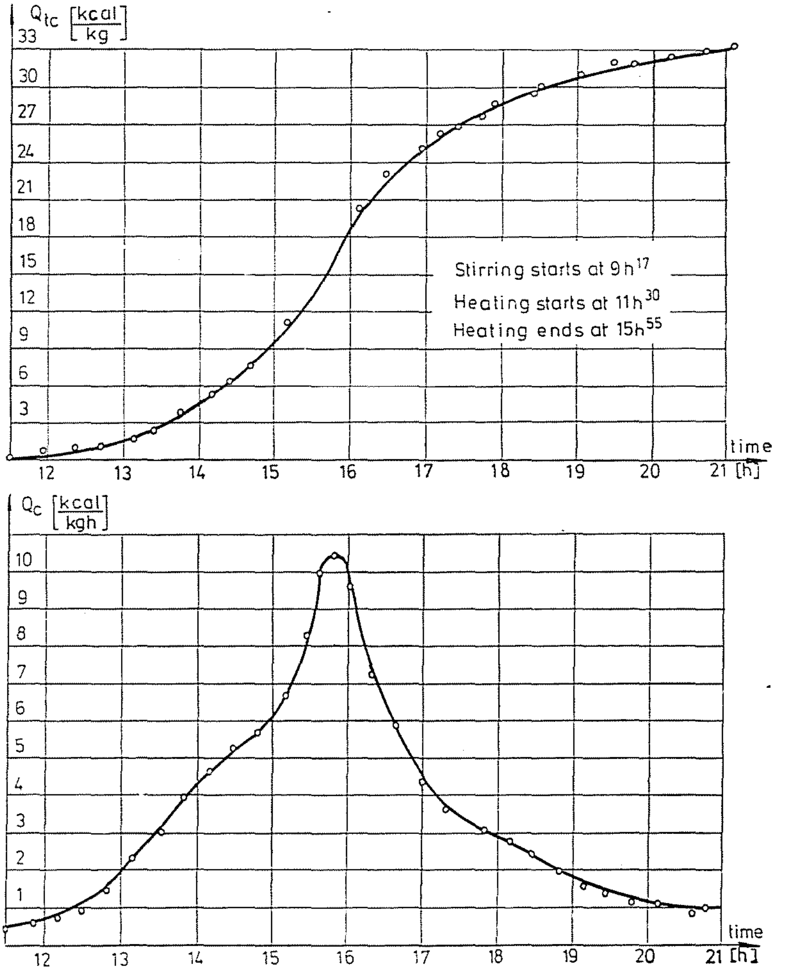

Fig. 8. Development and rate of hydration development of Portland cement C 500 DCM throughout steam-curing in test 4. (Initial temperature 25.18 °C, final temperature 73.4 °C)

fer test, the effect of the steel shuttering was completely neglected, in conformity with the literature. It was established that as long as steam is condensating on the surface of the units in the heat-up period, the conductivity ranges from 100 to 300 kcal/m^2 · hour · °C, while it is only 10 to 20 kcal/m^2 · hour · °C in the cooling period, depending on the air motion and the relative humidity.

Because of uncertainties in the determination of thermal characteristics, the effect of varying each factor was checked by computer.

Figs 2, 3, 4 and 5 show variation of specific heat and density of the concrete not to significantly affect the development of tensile stress maxima,

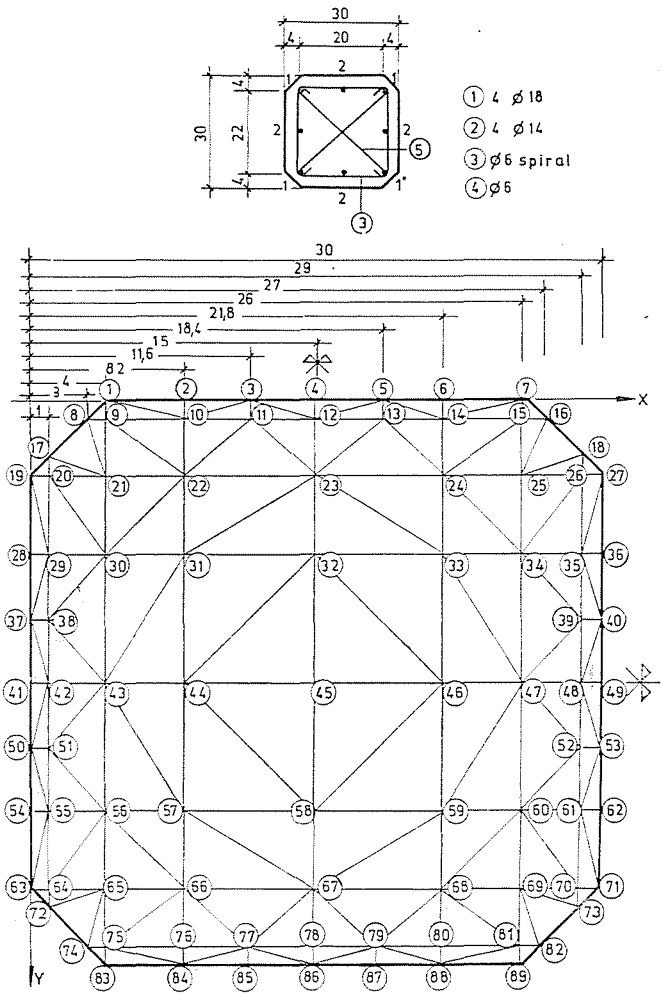

Fig. 9. Reinforcement in column NC-80 and triangle division used for calculating the thermal stresses

though the conductivity and heat transfer coefficients considerably influenced the stress development. The triangular division and the steam-curing diagram used for the computation are shown in Fig. 6. The concrete heat expansion coefficient adopted was that of PALOTÁS [2]. Since no adequate data were available in the literature for hydration heat development in steam-curing conditions, direct experiments were made, using test equipment shown in Fig. 7. In Fig. 8 the diagrams of cement hydration heat development and heat release rate are plotted for one of the five tests carried out.

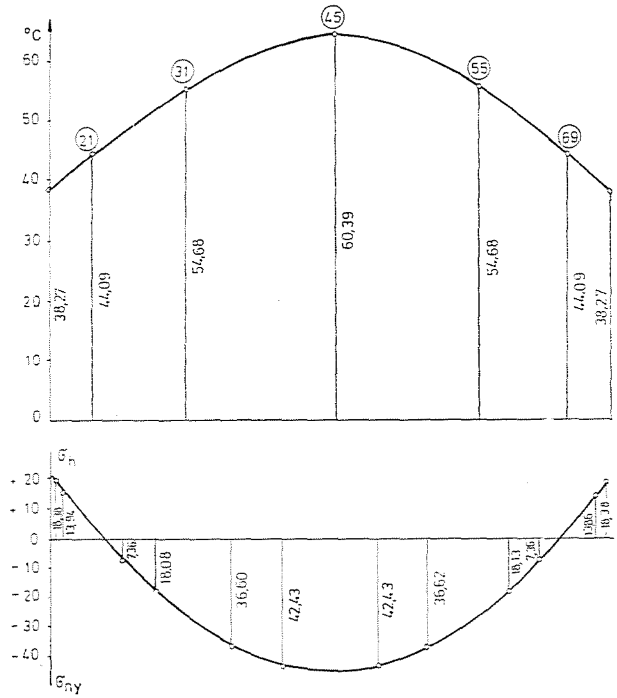

Fig. 10. Temperature and stress distribution in the diagonal section of the column NC-80 90 min after taken out of the steam-curing chamber

The computer outputs show a good agreement with test results obtained at the Department of Building Materials in 1968.

Stresses due to uneven temperature distribution in two products of the Concrete and Reinforced Concrete Works were tested assuming that the steam-curing diagrams in the technological specification have been observed. The two members (reinforced concrete column Y 46 A and reinforced concrete pile NC-80) were steam-cured according to the same diagram. The thermal stresses obtained by the computer, however, differed very much. This shows that in establishing the technology for some mass-produced unit, optimum cooling conditions should be considered. Computations reveal also damages likely to result from the neglection of technological specifications.

Figs 9, 10 show the reinforced concrete pile NC-80, the applied triangular division and the distribution of temperatures and stresses σ_z along the diagonal.

Figs 11, 12 show the cross-section of the reinforced concrete column, the applied division and the isotherm lines of the temperature field of the column 1 1/2 h after leaving the chamber. Concrete tensile strength values of the pile and the column were assessed according to HELLMANN [3] and it could be stated that the

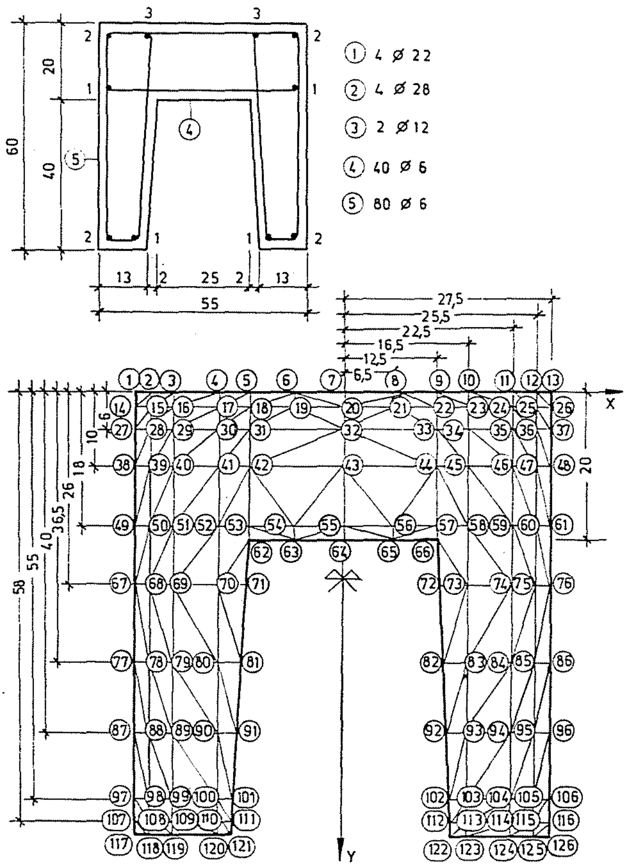

Fig. 11. Reinforcement in column Y 46 A and triangle division used for calculating the thermal-stresses

tensile strength of the pile was not reached, whereas in the corner region of the reinforced concrete column the tensile stress values were over twice the tensile strength. Here cracks occur by all means. The tests proved to be a good practice not to wet the elements immediately after stripping, because this increased the heat transfer factor and contributed to the uneven heat distribution, likely to cause stresses many times higher than those due to shrinkage.

The described computerized method lends itself to further improve the steam-curing technology for large-size units; outcomes of the kind would be of special use in developing the technology for the recently installed automatic steam control devices.

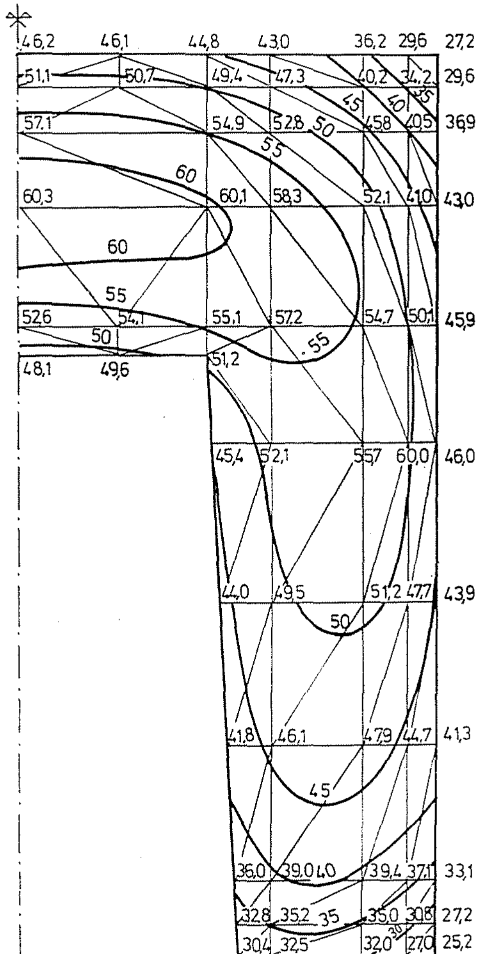

Fig. 12. Isotherms of the temperature field in the cross-section of column Y 46 A, 90 min after taken out of the steam-curing chamber

Summary

Determination of thermal stresses arising in precast r. c. products in the cooling period of steam curing has been set as an objective, in order to prevent cracking due to erroneous steam curing parameters. A computerized method has been developed, based on the method of finite elements, to determine the temperature distribution, or better, the thermal stresses in beams of arbitrary cross-section. Computer outputs and conclusions drawn thereof are presented. Thermal characteristics as inputs have been taken from the literature, and the setting heat development process has been experimentally studied.

References

1. BALÁZS, GY.—ZIMONYI, GY.—ZOBEL: Stresses and cracks in precast concrete due to uneven temperature distribution* Mélyépítéstudományi Szemle, 1967, No. **6.**
2. PALOTÁS, L.: Inherent concrete stresses due to temperature changes* Mélyépítéstudományi Szemle, 1970, No. **8.**
3. HELLMANN: Beziehungen zwischen Zug- und Druckfestigkeit des Betons. Beton, 1969, No. **2.**

Ass. Prof. Dr. György BALÁZS, } 1111 Budapest, Műegyetem rkp. 3.
Ass. Béla SZENTIVÁNYI }
Miklós BERÉNYI, section head, 1052 Budapest, Martinelli tér 3. Hungary

* In Hungarian